Check for updates

Advanced Optical Materials

ADVANCED OPTICAL MATERIALS
www.advopticalmat.de

RESEARCH ARTICLE OPEN ACCESS

Highly Efficient Pure-Blue Single-Layer Organic Light-Emitting Diodes Without High-Triplet-Energy Auxiliary Materials

Xiao Tan[1] | Manish Kumar[2] | Oskar Sachnik[1] | Rishabh Saxena[1] | Paul W. M. Blom[1] | Gert-Jan A. H. Wetzelaer[1]

[1]Max Planck Institute for Polymer Research, Mainz, Germany | [2]Dr. Manish Kumar, Department of Mechanical and Materials Engineering, University of Turku, Turku, Finland

Correspondence: Manish Kumar (manish.kumar@utu.fi) | Gert-Jan A. H. Wetzelaer (wetzelaer@mpip-mainz.mpg.de)

Received: 16 October 2025 | **Revised:** 6 March 2026 | **Accepted:** 10 March 2026

Keywords: charge transport | hyperfluorescence | organic light-emitting diodes | pure-blue emission | thermally activated delayed fluorescence

ABSTRACT

Blue organic light-emitting diodes (OLEDs) utilizing triplet-harvesting emitters require the use of high-triplet-energy hosts and blocking layers to confine the triplet excitons to the emitter. The use of these materials poses design challenges, while potentially compromising charge transport and operational stability. Here, we present efficient single-layer blue OLEDs comprising solely of a neat thermally activated delayed fluorescence (TADF) emitter sandwiched between two charge-injecting electrodes, without using high-triplet-energy materials. By further incorporating a narrow-band terminal emitter, we simultaneously improve the charge balance and color purity, realizing pure-blue single-layer hyperfluorescent OLEDs with an external quantum efficiency (EQE) of 21.1% and minimal efficiency roll-off. Analysis of the charge transport reveals that the improvement in charge balance is caused by the offset in ionization energy between the TADF sensitizer and the terminal emitter, slowing down hole transport. Our results demonstrate the feasibility of efficient pure-blue single-layer OLEDs without auxiliary high-triplet-energy materials, featuring a simple design and added stability benefits.

1 | Introduction

Organic light-emitting diodes (OLEDs) represent a promising technology for next-generation light sources and are well established in high-end displays, owing to their superior color rendering, thinness, low power consumption, and their compatibility with flexible displays [1]. However, current blue OLEDs based on triplet-harvesting emitters still lack sufficient operational stability, hindering their use in commercial applications [2]. In addition, highly efficient OLEDs usually consist of a multilayer stack comprising several charge-transport and blocking layers, in order to confine the excitons and charges to the emissive layer [3]. Apart from the fact that such multilayer OLEDs are difficult to design, for blue OLEDs, the necessary high-triplet-energy (E_T) host materials and blocking layers potentially contribute to device degradation [4, 5]. Furthermore, from a research perspective, analyzing the device physics and identifying the cause of degradation within a complex multilayer stack is challenging [6].

Recently, highly efficient single-layer OLEDs based on TADF emitters were realized as promising alternatives. Such single-layer OLEDs do not contain charge-transport or blocking layers, offering advantages in terms of design, fabrication, and operational stability [6–8]. In particular, single-layer OLEDs have been demonstrated to be fundamentally more stable than their multilayer counterparts, as the broad recombination zone inside the active layer reduces the density of excitons

This is an open access article under the terms of the Creative Commons Attribution License, which permits use, distribution and reproduction in any medium, provided the original work is properly cited.

© 2026 The Author(s). *Advanced Optical Materials* published by Wiley-VCH GmbH

and polarons, the interaction between which is believed to be the main cause of device degradation under operation. Highly reactive excitons and polarons can be generated by the exciton annihilation events, such as triplet-triplet (TTA) and triplet-polaron (TPA) interactions, which are capable of attacking the chemical bonds, with the resulting fragments causing charge traps during device operation [9]. In the presence of blocking layers, charges and excitons may accumulate at the interfaces, increasing their interactions and accelerating degradation. Indeed, the choice of interface materials surrounding the emissive layer has been shown to play a crucial role in degradation [10–13].

Recently, we have demonstrated a highly efficient sky-blue OLED in a single-layer structure [8]. Although a virtually 100% internal quantum efficiency was achieved without charge- or exciton-confinement layers, a high-triplet-energy host material was still required. Furthermore, as is common with TADF emitters due to the charge-transfer character of the excited states, the emission spectrum was broad, compromising color purity.

To obtain a narrow emission spectrum while still harvesting triplet excitons via TADF, the concept of hyperfluorescence has been introduced [14, 15]. In this concept, the excited stated created on the TADF sensitizer is transferred to a fluorescent terminal emitter with a narrow emission spectrum via Förster resonance energy transfer (FRET). By using a low concentration of the terminal emitter, typically around 1%, short-range Dexter transfer of triplet excitons can be minimized [16].

However, since the terminal emitter is required to have a smaller bandgap than the TADF sensitizer, the addition of such fluorescent emitter is expected to cause unintended charge trapping of either electrons, holes, or both. It is known that charge trapping can drastically reduce the charge transport in organic semiconductors, even if the concentration of charge traps is in the order of only 10^{23} m^{-3}, which equates to a relative concentration of only 0.01%–0.1% [17, 18]. Surprisingly, this fundamental issue with hyperfluorescence has been hardly addressed to date. Only a qualitative effect of charge trapping has been reported without systematic analysis of the charge transport [19, 20]. Recently, it was demonstrated that charge trapping in a hyperfluorescent OLED can be avoided in case the energy levels of the terminal emitter are within the energetic disorder of charge transport states of the host and/or sensitizer [21]. However, it is still unclear if strategical trapping on the terminal emitter can be used to positively influence the charge balance in hyperfluorescent OLEDs.

Here, we demonstrate efficient pure-blue single-layer OLEDs based on hyperfluorescence, without the use of high triplet energy auxiliary materials. By using a terminal emitter with a lower ionization energy than the neat TADF matrix, the hole transport is slowed down, improving the charge balance compared to the hole-dominant neat TADF emitter. Balancing the charge transport upon optimizing the terminal-emitter concentration leads to increased OLED efficiencies. As a result, EQEs of above 20% are demonstrated for single-layer pure-blue OLEDs, without host, charge-transport, or charge- and exciton blocking materials.

2 | Results and Discussion

As a first step, the blue TADF emitter DMAC-DPS (10,10′-(4,4′-sulfonylbis(4,1-phenylene))bis(9,9-dimethyl-9,10-dihydroacridine)) was selected. This emitter exhibits an electroluminescence peak at 480 nm and demonstrates excellent concentration-insensitive properties, with a photoluminescence quantum yield (PLQY) of 0.88 in the neat film [22]. Single-layer OLEDs based on DMAC-DPS were fabricated with a device structure of ITO/PEDOT:PSS:PFI/DMAC-DPS(92 nm)/Ba(5 nm)/Al (100 nm) (inset in Figure 1a). Essentially, the emissive layer (DMAC-DPS) is directly sandwiched between the anode and cathode, without employing any high triplet energy surrounding layers for exciton or charge confinement. The spin-coated PEDOT:PSS:PFI (poly(3,4-ethylenedioxythiophene):polystyrene sulfonate: perfluorinated ionomer) film exhibits a high work function of 5.9 eV and forms an ohmic hole contact with DMAC-DPS, which has an ionization energy (IE) of 5.9 eV, as shown in Figure S1 and is consistent with previous results [8]. Owing to the efficient charge injection, our single-layer OLED with a pristine DMAC-DPS emissive layer showed a maximum EQE of 19.2% (Figure 1b), without using high E_T functional layers. The device exhibited sky-blue electroluminescence at 490 nm with CIE1931 coordinates of (0.16, 0.36). Due to the ohmic charge injection directly into the emissive layer, low operating voltages were achieved, with a turn-on voltage of only 2.8 V, leading to a high luminous efficacy of 43 lm/W. For comparison, a reported single-layer OLED with a neat DMAC-DPS emissive layer showed an EQE_{max} of only 0.11% [10], which we ascribe to the used (non-ohmic) contacts. By contrast, reported multilayer OLEDs based on neat DMAC-DPS showed an EQE of up to 19.5% by including a high E_T charge and exciton confinement layer, which, however, increased the operating voltage, resulting in a lower luminous efficacy of 19 lm/W [10]. Our results, therefore, demonstrate that high-efficiency TADF OLEDs are feasible even without any high E_T auxiliary materials.

To understand the outstanding performance of this simple blue OLED, we investigated the charge transport characteristics of the emitter. In a single-layer OLED, charge balance is exclusively determined by the charge-transport properties of the emissive layer. Therefore, we fabricated hole-only (HOD) and electron-only (EOD) devices of DMAC-DPS films sandwiched between ohmic contacts. In Figure S2, the measured current density versus voltage (*J-V*) characteristics of the single-carrier devices are compared. At high voltages, the hole and electron current are close to each other, indicating quite balanced charge transport. However, at lower voltages, the electron current is clearly lower and exhibits a stronger voltage dependence than the hole current. This implies that the electron transport is trap limited, which is common for organic semiconductors with a low electron affinity (EA) [23]. The charge transport was quantified by fitting the temperature-dependent current-voltage characteristics with drift-diffusion simulations incorporating the extended Gaussian disorder model for the mobility [24, 25]. We obtained a zero-field and zero-density hole mobility of 2.4×10^{-12} m^2 V^{-1} s^{-1}. The electron mobility at zero field and density amounted to 6.9×10^{-12} m^2 V^{-1} s^{-1}, which is comparable to the hole mobility. However, the electron transport is additionally hindered by deep

21951071, 0, Downloaded from https://advanced.onlinelibrary.wiley.com/doi/10.1002/adom.202503375 by University of Turku, Wiley Online Library on [25/03/2026]. See the Terms and Conditions (https://onlinelibrary.wiley.com/terms-and-conditions) on Wiley Online Library for rules of use; OA articles are governed by the applicable Creative Commons License

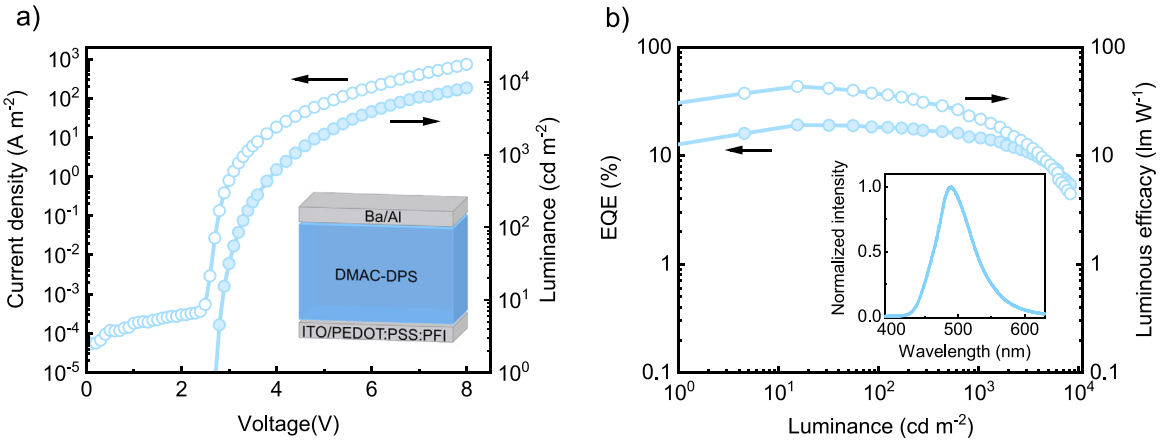

FIGURE 1 | Device performance of a single-layer DMAC-DPS OLED with no high E_T materials. a) Current density-voltage and luminance-voltage characteristics of a DMAC-DPS OLED with an emissive layer thickness of 92 nm. The inset shows the device structure. b) EQE and luminous efficacy versus luminance with the electroluminescence spectrum displayed in the inset.

electron traps with a density of 8×10^{22} m^{-3}, which makes DMAC-DPS a hole-dominated emitter. To summarize, the high EQE of the single-layer DMAC-DPS OLEDs can be explained by the ohmic charge injection and the fairly balanced mobilities, but the presence of electron trapping demonstrates that there is still room for improvement with regard to charge balance.

The demonstration of 19% EQE in a single-layer blue OLED shows that high efficiency is feasible without any high E_T materials. However, the EL spectrum of DMAC-DPS has a full width at half maximum (FWHM) of 62 nm, which compromises color purity. Therefore, we incorporated the multi-resonance TADF material ν-DABNA into the emissive layer as a narrow-band blue terminal emitter [26], which has a singlet excited state S_1 of 2.65 eV and can be excited by energy transfer from DMAC-DPS ($S_1 = 2.7$ eV) [22]. ν-DABNA has a photoluminescence peak at 468 nm and a FWHM of 14 nm in toluene solution [26]. For a single-layer OLED based on DMAC-DPS doped with a small concentration of ν-DABNA, the energy-level diagram is shown in Figure 2. Since the IE of ν-DABNA (5.4 eV) [26] is lower than the IE of DMAC-DPS (5.9 eV) [22], it is expected that this terminal emitter causes hole trapping, while the electron transport should not be affected based on the energy levels.

To verify hole trapping by ν-DABNA experimentally, we fabricated HODs and EODs of DMAC-DPS with different doping concentrations of ν-DABNA. The *J-V* characteristics of the HODs are displayed in Figure 3a. It is evident that the hole current drops by a factor of 20, just by incorporating 0.5% of ν-DABNA. This clearly demonstrates hole trapping on the ν-DABNA molecules. By increasing the ν-DABNA concentration, the hole current drops further, which is expected with an increasing hole-trap concentration. To quantify the amount of hole traps due to the incorporation of ν-DABNA, the hole currents were fitted with drift-diffusion simulations, based on the charge-transport parameters for pristine DMAC-DPS and including additional hole traps. The hole traps were assumed to be distributed in energy according to a Gaussian with a width of 0.1 eV. The hole-trap depth was determined to be 0.51 eV, corresponding well to the IE offset between DMAC-DPS and ν-DABNA. It should be noted that the *effective* trap depth is noticeably smaller [21], because of the

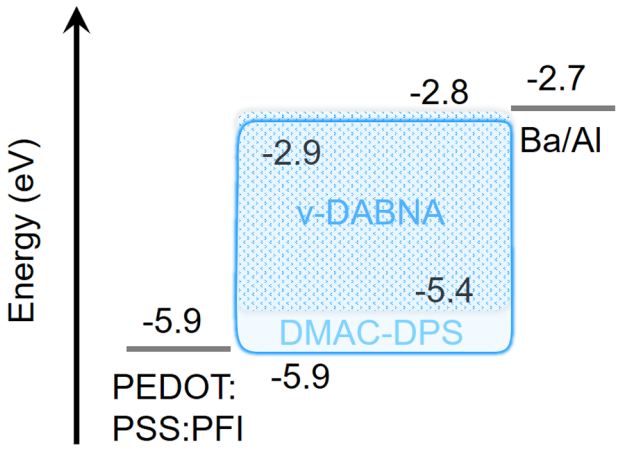

FIGURE 2 | Energy level diagram of the single–layer hyperfluorescence OLED. The emissive layer consists of ν-DABNA doped in DMAC-DPS and is sandwiched between an ohmic anode (PEDOT:PSS:PFI) and a Ba/Al cathode. The PEDOT:PSS:PFI layer aligns well with the HOMO level of DMAC-DPS (−5.9 eV), enabling efficient hole injection, while the Ba/Al cathode allows electron injection into the LUMO (−2.9 eV), forming a complete device without the need for additional charge transport or blocking layers.

high energetic disorder ($\sigma = 0.15$ eV, as determined from the hole-transport simulations) of the density-of-states (DOS) distribution of DMAC-DPS. This is taken into account in the drift-diffusion simulations by subtracting a value of $\sigma^2/(2kT)$ (where k is the Boltzmann constant and T is the temperature) from the absolute trap depth of 0.51 eV. Effectively, the mean hole-trap depth is only 0.07 eV, with a variance due to the assumed width of the Gaussian trap-DOS distribution.

The extracted hole-trap densities are displayed in the inset of Figure 3a. The hole-trap density was determined to be 1.8×10^{24} m^{-3} for a doping concentration of 0.5% of ν-DABNA. In the simulations, a hopping distance of 1.4 nm for pristine DMAC-DPS, which corresponds to a density of states of 3.6×10^{26} m^{-3}. As a result, the extracted trap density 1.8×10^{24} m^{-3} equates to a relative trap concentration of 0.5%, practically the same as

21951071, 0, Downloaded from https://advanced.onlinelibrary.wiley.com/doi/10.1002/adom.202503375 by University of Turku, Wiley Online Library on [25/03/2026]. See the Terms and Conditions (https://onlinelibrary.wiley.com/terms-and-conditions) on Wiley Online Library for rules of use; OA articles are governed by the applicable Creative Commons License

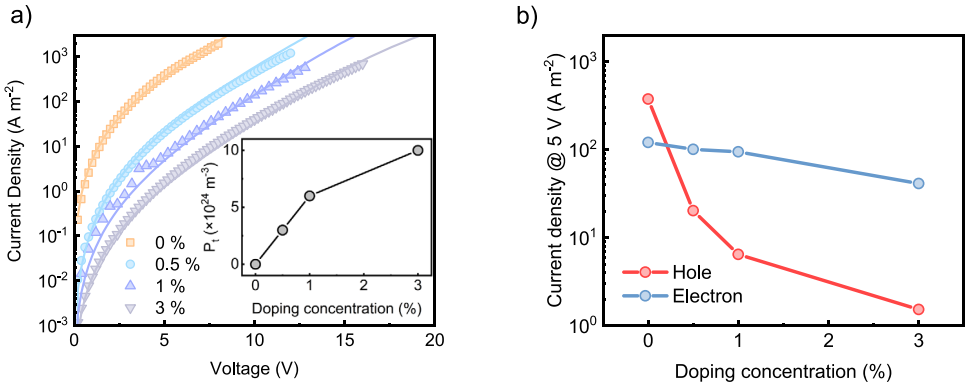

FIGURE 3 | Charge transport in DMAC-DPS as a function of the ν-DABNA doping concentration. a) Current density-voltage characteristics of HODs at different doping concentrations (symbols). Solid lines are the corresponding drift-diffusion simulations, with the use hole-trap concentration displayed in the inset. b) Current density in HODs and EODs at a voltage of 5 V (corrected by the built-in voltage of 0.5 V for EODs). The thickness of the active layers of both HODs and EODs are 94 nm (0%), 101 nm (0%), 101 nm (1%), and 103 nm (3%).

the doping concentration of ν-DABNA. For a high ν-DABNA concentration of 3%, the modeled trap density is lower than expected, which could be due to the nature of ν-DABNA to aggregate [27], implying that one trap site corresponds to multiple ν-DABNA molecules. Such aggregation-induced quenching is also confirmed by the reduction in PLQY between the 0.5% doped film (90%) and the 3% doped film (63%). The variation of the hole current over two orders of magnitude upon doping demonstrates the high sensitivity of the charge transport even to small concentrations of terminal emitters, even despite the very shallow effective hole-trap depth in this case.

In contrast to the hole currents, the electron currents are only marginally affected by doping with ν-DABNA, as displayed in Figure S3,. Figure 3b shows the electron and hole current density at 5 V, as a function of the doping concentration. While there is a large drop in the hole current densities due to hole trapping on ν-DABNA, the electron current density remains stable, which means that ν-DABNA has almost no effect on the electron transport of DMAC-DPS. This implies that doping with ν-DABNA can shift the charge balance from hole dominated to electron dominated in DMAC-DPS.

Recently, we have demonstrated that shifting the recombination zone away from the metal electrode improves the EQE in single-layer OLEDs due to improved light outcoupling [28]. Since doping ν-DABNA into DMAC-DPS shifts the charge balance from hole dominated to electron-dominated, we would expect charge recombination to take place closer to the anode, thereby improving optical outcoupling. To confirm this, single-layer OLEDs of DMAC-DPS with different ν-DABNA doping concentrations were fabricated. Figure 4 shows the current density-voltage-luminance (*J-V-L*), EQE as function of luminance, and EL spectra, with the performance metrics listed in Table 1.

First of all, the hyperfluorescent OLEDs exhibit narrow-band blue emission with an FWHM of 21 nm, confirming full energy transfer from DMAC-DPS to ν-DABNA. Near complete energy transfer was also observed in steady-state PL experiments (Figure S9). The OLED doped with 0.5% ν-DABNA achieves the highest EQE of 21.1%, still remaining at 18.9% at a brightness of 1000 cd m^{-2}, which demonstrates both improved efficiency and lower roll-off compared to neat DMAC-DPS. We conjecture that the small roll-off is caused by the high-energy excitons being largely consumed by ν-DABNA through radiative decay rather than participating in annihilation processes that reduce the efficiency at high brightness. The device exhibited a pure blue color with chromaticity coordinates of CIE1931(x, y) (0.12, 0.17), compared to the sky-blue color of pristine DMAC-DPS (0.16, 0.36). Regarding the other doping concentrations, the EQE characteristics of the OLED with 1% ν-DABNA concentrations are fairly similar, whereas the EQE_{max} decreases to 15.3% for a 3% doping concentration.

Potentially, at 3% doping ratio, hole trapping becomes so severe that free charges would recombine directly on ν-DABNA rather than FRET energy transfer from the DMAC-DPS sensitizer. In this scenario, DMAC-DPS would no longer be electrically excited for higher ν-DABNA concentrations, which is in line with the operational stability measurements on these OLEDs, as reported in Table 1. With increasing ν-DABNA concentration, the lifetime of the OLEDs improves substantially. As DMAC-DPS is a very unstable emitter with low bond-dissociation energies [29], transferring the excited state to ν-DABNA leads to considerable lifetime improvements. At a ν-DABNA concentration of 3% though, the lifetime improvement comes at the expense of quantum efficiency and driving voltage, the latter being the result of heavy hole trapping. The slight shift in peak emission wavelength further confirms the tendency of ν-DABNA to aggregate at higher doping concentrations [30] and exhibit concentration quenching, which may also be responsible for the lower PLQY (63%).

In fact, the drop in PLQY for 3% ν-DABNA doping can fully explain the reduced EQE_{max} of 15.3%. The optical outcoupling in a single-layer OLED is expected to increase for a recombination zone shifting away from the metal cathode [28]. Therefore, the shift from a hole-dominated to an electron-dominated device upon ν-DABNA doping first increases the EQE via improved outcoupling, whereas the reduced EQE at higher ν-DABNA loading is mainly an effect of a reduced PL efficiency due to concentration quenching. Overall, we here demonstrate that the position of the recombination zone can be controlled by modifying the charge transport by adding a dopant, whereas the position usually depends on the intrinsic charge transport of the emitter in single-layer OLEDs [28].

21951071, 0, Downloaded from https://advanced.onlinelibrary.wiley.com/doi/10.1002/adom.202503375 by University of Turku, Wiley Online Library on [25/03/2026]. See the Terms and Conditions (https://onlinelibrary.wiley.com/terms-and-conditions) on Wiley Online Library for rules of use; OA articles are governed by the applicable Creative Commons License

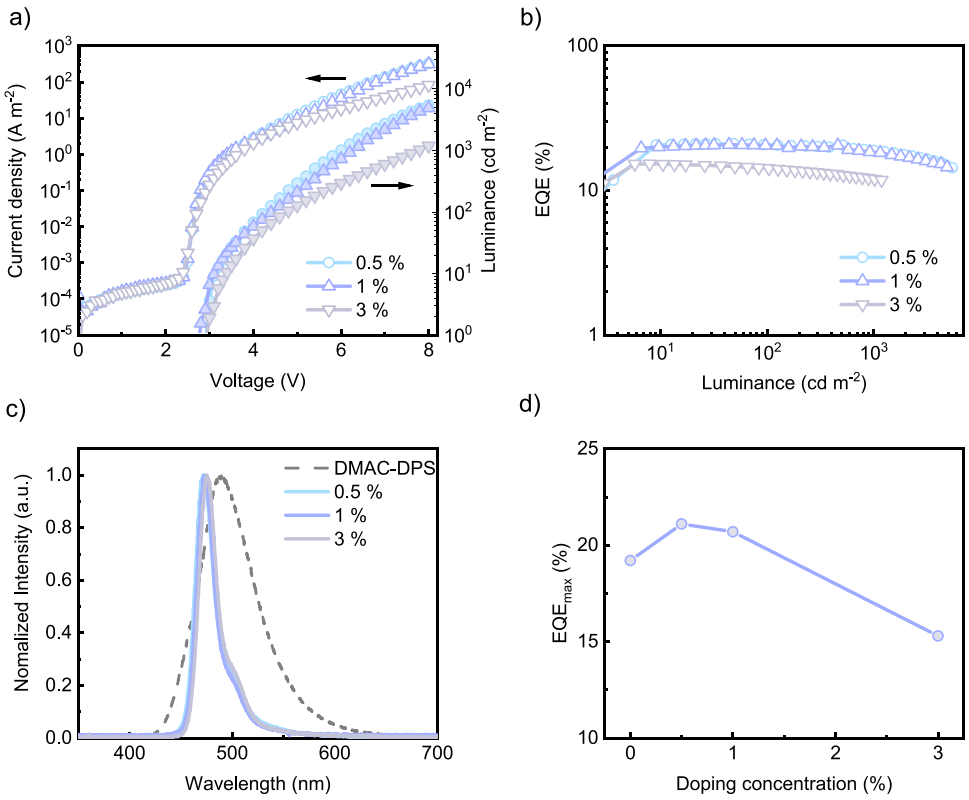

FIGURE 4 | OLED performance of hyperfluorescent OLEDs at different ν-DABNA doping concentrations. a) Current density-voltage and luminance-voltage characteristics. b) EQE as a function of luminance. c) Normalized EL spectra, with the EL spectrum of neat DMAC-DPS as a reference (dashed line). d) Maximum EQE of OLEDs versus doping concentration (%).

TABLE 1 | Performance metrics of DMAC-DPS single-layer OLEDs as a function of ν-DABNA doping concentration.

Doping concentration	V_{on} [V][a)]	EQE_{max} [%]	EQE_{100} [%][b)]	EQE_{1000} [%][c)]	λ_{EL} [nm][d)]	FWHM [nm][e)]	LT_{50} [min][f)]	CIE (x,y)
0%	2.8	19.2	18.3	14.5	490	62	0.5	0.16,0.36
0.5%	2.9	21.1	20.7	18.9	471	21	7	0.12,0.17
1%	2.8	20.7	20.5	18.2	473	21	18	0.12,0.18
3%	2.9	15.3	14.2	12.0	475	21	128	0.11,0.20

[a)]Turn-on voltage at 1 cd m^{-2}.
[b)]EQE at 100 cd m^{-2}.
[c)]EQE at 1000 cd m^{-2}.
[d)]EL peak wavelength.
[e)]FWHM of EL spectrum.
[f)]device lifetime to 50% of the initial luminance under constant current stress of 10 A m^{-2}, corresponding to a luminance of around 200 cd m^{-2}.

3 | Conclusions

In summary, we have demonstrated efficient pure-blue single-layer OLEDs without employing high-triplet-energy auxiliary materials. First, simple blue OLEDs based on a single layer of neat DMAC-DPS sandwiched between two electrodes were demonstrated. Subsequently, the broad emission spectrum of DMAC-DPS was narrowed by adding a low concentration of the MR-TADF emitter ν-DABNA as a terminal emitter. Due to shallow hole trapping on ν-DABNA, the charge balance is improved, leading to simple-structure pure-blue OLEDs with an EQE of up to 21% and low efficiency roll-off. Balancing the charge transport avoids the use of high triplet energy blocking layers, which frequently compromise operating voltage and

21951071, 0, Downloaded from https://advanced.onlinelibrary.wiley.com/doi/10.1002/adom.202503375 by University of Turku, Wiley Online Library on [25/03/2026]. See the Terms and Conditions (https://onlinelibrary.wiley.com/terms-and-conditions) on Wiley Online Library for rules of use; OA articles are governed by the applicable Creative Commons License

stability. While the stability of the OLEDs presented here is still rather low due to the instability of DMAC-DPS, our results demonstrate that efficient host-free pure-blue single-layer OLEDs are feasible, minimizing the number of components of the organic-layer stack.

4 | Experimental Section

4.1 | Materials

Nafion (PFI) was purchased from Sigma–Aldrich as 5 wt.% solution in a mixture of lower aliphatic alcohols and water, containing 45% water. ν-DABNA and DMAC-DPS were purchased in sublimed grade from Ossila BV.

4.2 | Device Fabrication

OLED devices were fabricated on ITO, which was pre-patterned on top of glass substrates. The substrates were cleaned by ultrasonication in acetone (5 min) and isopropyl alcohol (5 min) each, followed by UV–ozone treatment (50 min). PEDOT: PSS: PFI blends were prepared by mixing PEDOT:PSS (CLEVIOS P VP AI 4083) with Nafion in a 1:6:14 ratio by wt. and diluted in deionized water (1:1), stirring it overnight. PEDOT:PSS:PFI was spin coated on freshly UV-treated ITO substrates and annealed at 130°C for 12 min, resulting in films of ∼20 nm thickness. The substrates were then transferred to a high vacuum chamber for thermal evaporation of the emissive layer under an operation pressure of 2×10^{-6} to 3×10^{-6} mbar. Barium (5 nm) and aluminum (100 nm) were evaporated consecutively to build the top electrode. For hole-only devices, a top contact consisting of C_{60} (4 nm), MoO_3 (10 nm), and aluminum (100 nm) was evaporated. For electron-only devices, aluminum (30 nm) was vacuum deposited on cleaned glass substrates and exposed to air for 5 min oxidation, followed by thermal evaporation of the emissive layer, a TPBi (4 nm) interlayer, and a barium (5 nm) and aluminum (100 nm) top electrode.

4.3 | Measurements

Electrical characterization was carried out in a nitrogen-filled glovebox with a Keithley 2400 source meter, and light output was recorded with a Si photodiode with NIST-traceable calibration. The photodiode was placed close to (but not in contact with) the OLED to capture all photons emitted in a forward hemisphere, and no light was captured from the substrate edges. The EQE, the luminance, and power efficiency were calculated from the measured photocurrent, the device current, and the electroluminescence spectrum. Electroluminescence spectra were obtained with a USB4000-UV–VIS-ES spectrometer.

Acknowledgements

The authors acknowledge the technical support from Frank Keller, Sirma Koynova, Michelle Beuchel, Verona Maus, and Christian Bauer. Manish Kumar acknowledges funding from the Academy of Finland project (2023-25) Hyper-MOLED with a Decision number 348727. Rishabh Saxena acknowledges funding from Deutsche Forschungsgemeinschaft (DFG; project no. 547125865).

Open access funding enabled and organized by Projekt DEAL.

Funding

Deutsche Forschungsgemeinschaft (DFG project no. 547125865). The Academy of Finland project (2023-25) Hyper-MOLED with decision number 348727.

Conflicts of Interest

The authors declare no conflicts of interest.

Data Availability Statement

The data that support the findings of this study are available from the corresponding author upon reasonable request.

References

1. C. W. Tang and S. A. VanSlyke, "Organic Electroluminescent Diodes," *Applied Physics Letters* 51 (1987): 913–915, https://doi.org/10.1063/1.98799.

2. E. Tankelevičiūtė, I. D. W. Samuel, and E. Zysman-Colman, "The Blue Problem: OLED Stability and Degradation Mechanisms," *Journal of Physical Chemistry Letters* 15 (2024): 1034–1047, https://doi.org/10.1021/acs.jpclett.3c03317.

3. J. Kido, M. Kimura, and K. Nagai, "Multilayer White Light-Emitting Organic Electroluminescent Device," *Science* 267 (1995): 1332–1334, https://doi.org/10.1126/science.267.5202.1332.

4. Y. Wang, J. H. Yun, L. Wang, and J. Y. Lee, "High Triplet Energy Hosts for Blue Organic Light-Emitting Diodes," *Advanced Functional Materials* 31 (2021), https://doi.org/10.1002/adfm.202008332.

5. C. Poriel, C. Quinton, F. Lucas, J. Rault-Berthelot, Z.-Q. Jiang, and O. Jeannin, "Spirobifluorene Dimers: Understanding How the Molecular Assemblies Drive the Electronic Properties," *Advanced Functional Materials* 31 (2021): 2104980, https://doi.org/10.1002/adfm.202104980.

6. O. Sachnik, Y. Ie, N. Ando, X. Tan, P. W. M. Blom, and G.-J. A. H. Wetzelaer, "Single-Layer Organic Light-Emitting Diode With Trap-Free Host Beats Power Efficiency and Lifetime of Multilayer Devices," *Advanced Materials* 36 (2024): 2311892, https://doi.org/10.1002/adma.202311892.

7. N. B. Kotadiya, P. W. M. Blom, and G.-J. A. H. Wetzelaer, "Efficient and Stable Single-Layer Organic Light-Emitting Diodes Based on Thermally Activated Delayed Fluorescence," *Nature Photonics* 13 (2019): 765–769, https://doi.org/10.1038/s41566-019-0488-1.

8. O. Sachnik, Y. Li, X. Tan, J. J. Michels, P. W. M. Blom, and G.-J. A. H. Wetzelaer, "Single-Layer Blue Organic Light-Emitting Diodes With Near-Unity Internal Quantum Efficiency," *Advanced Materials* 35 (2023): 2300574, https://doi.org/10.1002/adma.202300574.

9. B. van der Zee, Y. Li, G.-J. A. H. Wetzelaer, and P. W. M. Blom, "Triplet-Polaron-Annihilation-Induced Degradation of Organic Light-Emitting Diodes Based on Thermally Activated Delayed Fluorescence," *Physical Review Applied* 18 (2022): 064002, https://doi.org/10.1103/PhysRevApplied.18.064002.

10. Q. Zhang, D. Tsang, H. Kuwabara, et al., "Nearly 100% Internal Quantum Efficiency in Undoped Electroluminescent Devices Employing Pure Organic Emitters," *Advanced Materials* 27 (2015): 2096–2100, https://doi.org/10.1002/adma.201405474.

11. G. F. Trindade, S. Sul, J. Kim, et al., "Direct Identification of Interfacial Degradation in Blue OLEDs Using Nanoscale Chemical Depth Profiling," *Nature Communications* 14 (2023): 8066, https://doi.org/10.1038/s41467-023-43840-9.

12. H. Nakanotani, K. Masui, J. Nishide, T. Shibata, and C. Adachi, "Promising Operational Stability of High-Efficiency Organic Light-

21951071, 0, Downloaded from https://advanced.onlinelibrary.wiley.com/doi/10.1002/adom.202503375 by University of Turku, Wiley Online Library on [25/03/2026]. See the Terms and Conditions (https://onlinelibrary.wiley.com/terms-and-conditions) on Wiley Online Library for rules of use; OA articles are governed by the applicable Creative Commons License

Emitting Diodes Based on Thermally Activated Delayed Fluorescence," *Scientific Reports* 3 (2013): 2127, https://doi.org/10.1038/srep02127.

13. D. P.-K. Tsang, T. Matsushima, and C. Adachi, "Operational Stability Enhancement in Organic Light-Emitting Diodes With Ultrathin Liq Interlayers," *Scientific Reports* 6 (2016): 22463, https://doi.org/10.1038/srep22463.

14. H. Nakanotani, T. Higuchi, T. Furukawa, et al., "High-Efficiency Organic Light-Emitting Diodes With Fluorescent Emitters," *Nature Communications* 5 (2014): 4016, https://doi.org/10.1038/ncomms5016.

15. T. Furukawa, H. Nakanotani, M. Inoue, and C. Adachi, "Dual Enhancement of Electroluminescence Efficiency and Operational Stability by Rapid Upconversion of Triplet Excitons in OLEDs," *Scientific Reports* 5 (2015): 8429, https://doi.org/10.1038/srep08429.

16. A. Monkman, "Why Do We Still Need a Stable Long Lifetime Deep Blue OLED Emitter?," *ACS Applied Materials & Interfaces* 14 (2022): 20463–20467, https://doi.org/10.1021/acsami.1c09189.

17. H. F. Haneef, A. M. Zeidell, and O. D. Jurchescu, "Charge Carrier Traps in Organic Semiconductors: A Review on the Underlying Physics and Impact on Electronic Devices," *Journal of Materials Chemistry C* 8 (2020): 759–787, https://doi.org/10.1039/C9TC05695E.

18. Y. Li, B. van der Zee, G.-J. A. H. Wetzelaer, and P. W. M. Blom, "Optical Outcoupling Efficiency in Polymer Light-Emitting Diodes," *Advanced Electronic Materials* 7 (2021): 2100155, https://doi.org/10.1002/aelm.202100155.

19. C.-Y. Chan, M. Tanaka, Y.-T. Lee, et al., "Stable Pure-Blue Hyperfluorescence Organic Light-Emitting Diodes With High-Efficiency and Narrow Emission," *Nature Photonics* 15 (2021): 203–207, https://doi.org/10.1038/s41566-020-00745-z.

20. K. Zhang, X. Wang, Y. Chang, Y. Wu, S. Wang, and L. Wang, "Carbazole-Decorated Organoboron Emitters With Low-Lying HOMO Levels for Solution-Processed Narrowband Blue Hyperfluorescence OLED Devices," *Angewandte Chemie International Edition* 62 (2023), https://doi.org/10.1002/anie.202313084.

21. O. Sachnik, N. Kinaret, R. Saxena, et al., "Pure-Blue Single-Layer Organic Light-Emitting Diodes Based on Trap-Free Hyperfluorescence," *Nature Materials* 24 (2025): 1742–1748, https://doi.org/10.1038/s41563-025-02294-8.

22. Q. Zhang, B. Li, S. Huang, H. Nomura, H. Tanaka, and C. Adachi, "Efficient Blue Organic Light-Emitting Diodes Employing Thermally Activated Delayed Fluorescence," *Nature Photonics* 8 (2014): 326–332, https://doi.org/10.1038/nphoton.2014.12.

23. N. B. Kotadiya, A. Mondal, P. W. M. Blom, D. Andrienko, and G.-J. A. H. Wetzelaer, "A Window to Trap-Free Charge Transport in Organic Semiconducting Thin Films," *Nature Materials* 18 (2019): 1182–1186, https://doi.org/10.1038/s41563-019-0473-6.

24. L. J. A. Koster, E. C. P. Smits, V. D. Mihailetchi, and P. W. M. Blom, "Device Model for the Operation of Polymer/Fullerene Bulk Heterojunction Solar Cells," *Physical Review B* 72 (2005): 085205, https://doi.org/10.1103/PhysRevB.72.085205.

25. W. F. Pasveer, J. Cottaar, C. Tanase, et al., "Unified Description of Charge-Carrier Mobilities in Disordered Semiconducting Polymers," *Physical Review Letters* 94 (2005): 206601, https://doi.org/10.1103/PhysRevLett.94.206601.

26. Y. Kondo, K. Yoshiura, S. Kitera, et al., "Narrowband Deep-Blue Organic Light-Emitting Diode Featuring an Organoboron-Based Emitter," *Nature Photonics* 13 (2019): 678–682, https://doi.org/10.1038/s41566-019-0476-5.

27. K. Stavrou, A. Danos, T. Hama, T. Hatakeyama, and A. Monkman, "Hot Vibrational States in a High-Performance Multiple Resonance Emitter and the Effect of Excimer Quenching on Organic Light-Emitting Diodes," *ACS Applied Materials & Interfaces* 13 (2021): 8643–8655, https://doi.org/10.1021/acsami.0c20619.

28. X. Tan, D. Dou, L.-L. Chua, et al., "Inverted Device Architecture for High Efficiency Single-Layer Organic Light-Emitting Diodes With Imbalanced Charge Transport," *Nature Communications* 15 (2024): 4107, https://doi.org/10.1038/s41467-024-48553-1.

29. Q.-Y. Meng, R. Wang, Y.-L. Wang, et al., "Longevity Gene Responsible for Robust Blue Organic Materials Employing Thermally Activated Delayed Fluorescence," *Nature Communications* 14 (2023): 3927, https://doi.org/10.1038/s41467-023-39697-7.

30. H. S. Kim, H. J. Cheon, D. Lee, et al., "Toward Highly Efficient Deep-Blue OLEDs: Tailoring the Multiresonance-Induced TADF Molecules for Suppressed Excimer Formation and Near-Unity Horizontal Dipole Ratio," *Science Advances* 9 (2023): adf1388, https://doi.org/10.1126/sciadv.adf1388.

Supporting Information

Additional supporting information can be found online in the Supporting Information section.

Supporting File: adom71148-sup-0001-SuppMat.pdf.

21951071, 0, Downloaded from https://advanced.onlinelibrary.wiley.com/doi/10.1002/adom.202503375 by University of Turku, Wiley Online Library on [25/03/2026]. See the Terms and Conditions (https://onlinelibrary.wiley.com/terms-and-conditions) on Wiley Online Library for rules of use; OA articles are governed by the applicable Creative Commons License